applied sciences

MDPI

Article

Modeling and Experimental Verification of the Electrical Efficiency for Variable-Frequency Rolling Piston Compressor under Variable Suction Conditions

Zheming Cheng [1,2,*], Leren Tao [1], Lihao Huang [1] and Zhongyang Yu [1]

[1] Institute of Refrigeration and Cryogenics, University of Shanghai for Science and Technology, Shanghai 200093, China; cryo307@usst.edu.cn (L.T.); dongliguan301@163.com.cn (L.H.); czm880224@126.com.cn (Z.Y.)
[2] Construction Department, Zhoukou Normal University, Zhoukou 466700, China
* Correspondence: czm0224@163.com

Abstract: The frequency and the suction refrigerant state are complex in the actual operation of variable compressors, which leads to the variability of compressor performance under different operating conditions. The characterization and the modeling of the compressor have become hot research topics. For modeling, the electrical efficiency model of the compressor, which could be applied to the suction refrigerant state at both the superheated and the two-phase stages, the compressor frequency, the pressure ratio, and the evaporation temperature, is analyzed through experiments in this paper. The results show that the linear electrical efficiency decreases with the declining superheated temperature and the increasing suction vapor quality when the system is at the fixed and evaporating temperature. Moreover, the slope of the two-phase suction is above that of the superheated suction. In addition, the system's electrical efficiency at the fixed pressure ratio is inversely proportional to the evaporation temperature, and the electrical efficiency of the system at the fixed evaporating temperature is also inversely proportional to the pressure ratio. The higher the variation of the pressure ratio, the smaller the evaporation temperature influences. To demonstrate the precision of the model, the theoretical value is compared with a confirmatory experiment in this paper. The maximum relative error is 1.81%, and the minimum is 0.035%.

Keywords: variable-frequency compressor; electrical efficiency; modeling; two-phase

check for updates

Citation: Cheng, Z.; Tao, L.; Huang, L.; Yu, Z. Modeling and Experimental Verification of the Electrical Efficiency for Variable-Frequency Rolling Piston Compressor under Variable Suction Conditions. *Appl. Sci.* **2023**, *13*, 12992. https://doi.org/10.3390/app132412992

Academic Editors: Sébastien Poncet and Filipe Soares

Received: 11 September 2023
Revised: 30 November 2023
Accepted: 30 November 2023
Published: 5 December 2023

Copyright: © 2023 by the authors. Licensee MDPI, Basel, Switzerland. This article is an open access article distributed under the terms and conditions of the Creative Commons Attribution (CC BY) license (https://creativecommons.org/licenses/by/4.0/).

1. Introduction

In recent years, the research on refrigeration and heat pump systems has mainly focused on improving system efficiency, exploring suitable configurations to optimize performance, and identifying optimal control strategies. The performance of refrigeration and heat pump systems depends heavily on the compressor, their core component. Therefore, it is crucial to have an accurate and easy-to-use model for analyzing and predicting compressor performance [1]. Experts and scholars worldwide have extensively researched compressor models to achieve a common goal. There are currently three primary modeling methods in use: the geometry- and physics-based, the empirical, and the semi-empirical methods [2].

Several mathematical models of compressors that use physical and geometric principles have been developed by experts [3–15]. To accurately determine the change in the refrigerant state within the compressor chamber, a range of detailed compressor-related parameters, such as geometric shape, leakage, oil properties, and thermodynamics, must be taken into account. Unfortunately, these models require complex calculations, and obtaining precise data for the compressor can be quite challenging [16].

For the calculation and optimization of compressor performance in refrigeration and heat pump systems, the mathematical models relying on geometric and physical

theories are difficult and time-consuming to compute. In such instances, empirical and semi-empirical compressor models are better suited for the task. Among them, empirical models such as (DIN EN 12900:2013, 2013) [17] or (AHRI Standard 540 2015) [18] are more advanced. These models consider mass flow rate and power consumption as third-degree polynomial functions of evaporation and condensation temperatures. However, they are only applicable to fixed compressor speeds. On the other hand, machine learning-based compressor models are relatively popular but require a large amount of experimental data for support [19]. Additionally, empirical models have poor extrapolation capability and may result in significant calculation errors.

The reliability of the predictions in varying operating conditions is better with semi-empirical compressor models than with empirical models. Additionally, their computational cost is relatively low, making them more practical for integration into complex system models [1]. LI has established a semi-empirical model for constant-speed scroll compressors based on thermodynamic principles, and the model has been extended to include reciprocating piston compressors. The model calculates refrigerant mass flow rate, discharge temperature, and shaft power, with errors within 5% compared to experimental values [20]. LI has created models for different types of compressors, including variable-speed scroll, reciprocating, and rolling piston compressors. These models have been tested against experimental values, and the errors for calculated refrigerant mass flow rate, shaft power, and discharge temperature are all below 3%. This indicates that the models are highly accurate in predicting these important parameters. [21]. MOLINAROLI L et al. have developed a semi-empirical model that accurately predicts the performance of rolling piston compressors. The model was tested on four different compressors under various operating conditions with different refrigerants. The model's accuracy was verified with calculated errors of within ±5% for the refrigerant mass flow rate and compressor power [22]. Sun et al. have developed a theoretical-based explicit calculation model for jet-type variable-speed scroll compressors. The predicted values of the mass flow rate, input power, and discharge temperature have a deviation within ±10%, ±5%, and ±3 K, respectively, compared to the experimental data [23]. A semi-empirical model for reciprocating compressors has been developed by Santos et al. This model is based on fundamental principles and enables power consumption and mass flow rate predictions for both single-speed and variable-speed compressors. The level of accuracy of the model is notable, with errors between the predicted and experimental values that are within 10% [24]. A semi-empirical model for variable-speed scroll compressors has been developed by Guth et al. This model is based on physical laws and predicts values for volumetric efficiency, adiabatic efficiency, and the product of electrical and mechanical efficiencies. When compared to the experimental data, the deviations for these predicted values fall within the ranges of +2.3/−1%, +9.1/−5.3%, and ±4.95%, respectively. Similarly, the predicted values for the refrigerant mass flow rate and discharge temperature also have deviations within the ranges of +1/−1.1 g/s and +0.6/−0.8 K, respectively, compared to the experimental data. As for power consumption, the deviation is +55/−90 W when compared to the experimental data [25]. Sun et al. have developed a semi-empirical thermodynamic model for the volumetric efficiency and power consumption of reciprocating compressors. The predicted values for the compressor power consumption have an error of less than 1% compared to the experimental data [26].

However, the aforementioned models do not consider the impact of the suction state of the compressor (superheated suction and wet compression) on the compressor model. Additionally, wet compression can make the vapor compression refrigeration cycle with pure working fluid closer to the ideal Carnot cycle. When the suction dryness is low, the liquid droplets drawn into the compressor completely vaporize within a short time, thereby improving compressor performance and reducing discharge temperature [27]. The wet compression cycle offers the highest possible efficiency for thermodynamic cycles operating between two temperatures with a heat sink and heat source [28,29]. Therefore, the development of a wet compression model for compressors holds significant importance in the facilitation of system simulation and optimization.

In brief, there is a dearth of research on modeling variable-speed compressors that undergo fluctuations in suction states. The compressor frequency and refrigerant state at the suction port exhibit a complex pattern during operation, leading to significant variations in compressor performance across diverse operating conditions. Therefore, it is crucial to delve into its properties and to create compressor models to address this issue. Rolling piston compressors are low-capacity compressors that are characterized by their small size, light weight, low cost, and high performance. They are widely used in low-capacity refrigeration and heat pump systems [22], and establishing a mathematical model for them is particularly significant.

Therefore, this paper presents an in-depth analysis of the effects of multiple factors on the electrical efficiency of a variable-speed rolling piston compressor. The factors studied include compressor frequency, suction superheat, suction dryness, evaporation temperature, and compression ratio. Through rigorous experimentation, we determined the variation law of the electrical efficiency. Furthermore, we developed a reliable model for steady-state electrical efficiency that can be applied to both the wet compression and the superheated suction stages of the rolling piston compressor. This model was validated through experiments, ensuring its accuracy and usefulness in practical applications.

2. Material and Methods

2.1. Instruments and Equipment

The experimental setup of the variable-speed rolling piston refrigeration system is shown in Figure 1. The system is composed of various components, including a rolling piston compressor 1, a condenser 2, an electronic expansion valve 3, an evaporator 4, a subcooling device 5, and a refrigerant flow measurement device 6, as well as a cooling water and chilled water circulation system 18 and 19 and other relevant elements.

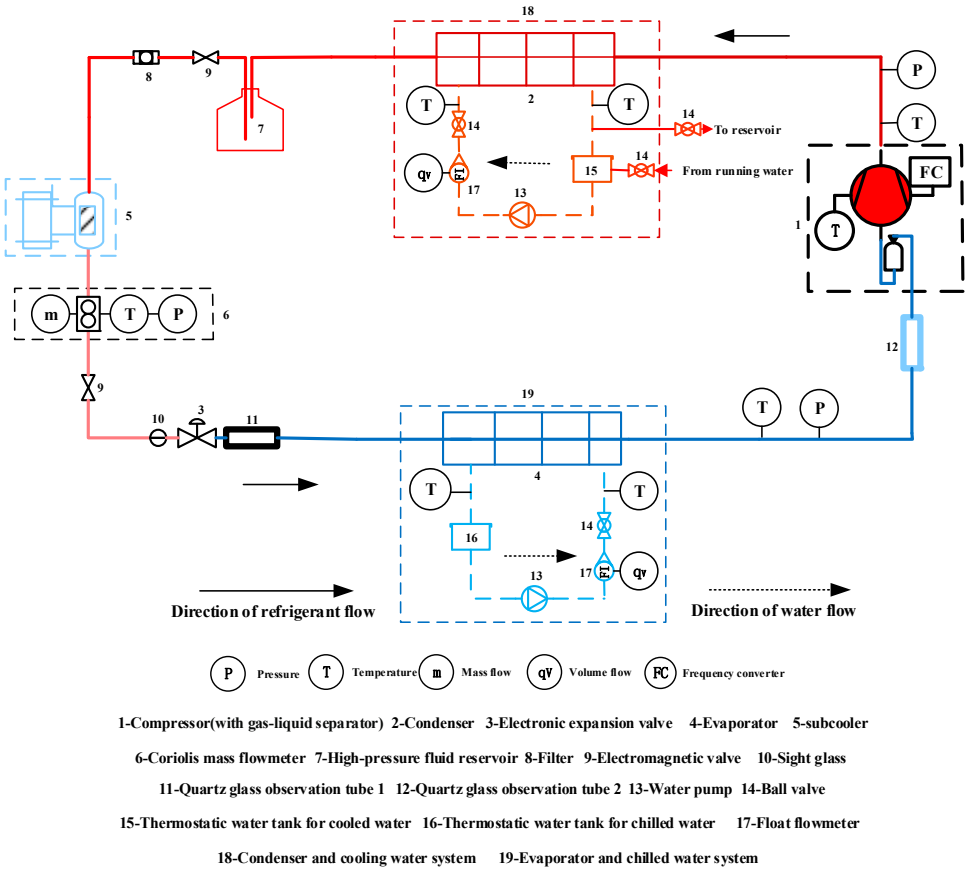


Figure 1. Schematic diagram of the experimental setup.

The compressor in this experimental setup is a variable-speed rolling piston compressor from Shanghai Hitachi, equipped with an internal gas–liquid separator. The compressor frequency can be set by a universal variable-frequency drive, with an adjustable frequency (f) range of 16.6 Hz to 120 Hz. The theoretical displacement volume V is 10.2 mL, and the compressor power consumption W is measured by a digital power meter. Both the evaporator and the condenser adopt compact brazed plate heat exchangers, where the heat exchange occurs between the refrigerant and the water. The refrigerant is R32, and the flow rate of the refrigerant, m_r, is measured by a Coriolis flow meter. The temperature T_v and pressure P_v of the refrigerant before the electronic expansion valve can also be measured. The subcooling degree of the refrigerant is controlled by the constant-temperature water tank 5. The opening value of the electronic expansion valve is manually controlled by a stepper motor. The condensation and evaporation temperatures are controlled by automatically adjusting the heating power of the water bath in the cooling water and the chilled water circulation system. The volume flow rate of chilled water, $q_{v,w}$, is measured by float flow meter 17, and the flow state of the refrigerant can be observed in sight glass 12.

T and P represent the temperature and pressure measurement points. The water inlet and outlet temperatures of the evaporator are denoted as $T_{w,i,}$ and $T_{w,o}$, respectively, while the suction and discharge temperatures of the compressor are denoted as T_{suc} and T_{dis}, respectively; these are all measured using built-in platinum resistors. The refrigerant outlet pressures of the evaporator and condenser are denoted as P_e and P_c, respectively, and are measured by pressure transmitters. The physical diagram of the experimental setup is shown in Figure 2. Table 1 provides details on the sensors and their corresponding uncertainties. The system operating parameters are collected by a Siemens S7-300 PLC programmable controller(SIEMENS, Berlin, Germany), and the cooling water and chilled water temperatures are controlled by PID. The data collected by the PLC are transmitted via data lines to the PC, monitored in real time, and reported on the human–machine interface based on the Sunway (ForceControlV6.0) configuration software development.



Figure 2. Actual diagram of the experimental setup.

Table 1. The experimental sensors and uncertainties.

Items	Products and Model	Manufacturer	Parameter Range	Uncertainties
Volume flow (L/min)	Rotameter (Z-4003)	USA General Electric Company (Boston, MA, USA)	4–36	±4%
Pressure (kPa)	Pressure transmitter (131AP5A2B2K1)	Danfoss China-Danfoss (Shanghai, China) Automatic Control Co. (Shanghai, China)	0–3500	±0.075%
Temperature (°C)	Thermal resistance (Pt100)	Shanghai Instrumentation & Automation Co. (Shanghai, China)	−10 to 125	±0.2 °C
Mass flow (kg/min)	Rheonik mass flowmeter (RHE08A1NNN)	China yuyao Zhenxing Flow Meter Factory (Ningbo, China)	0.25–5	±0.2%
Power (W)	Power meter	Shanghai Hongyin Electronic Technology Co. (Shanghai, China)	0–1000	±0.5%

2.2. Method and Design

The electrical efficiency of the rolling piston compressor is mainly influenced by parameters such as compressor frequency, suction ratio volume, compression ratio, suction superheat, etc. Therefore, the experimental scheme is designed using the method of controlled variables. The experimental scheme is shown in Table 2.

Table 2. Experimental scheme.

Serial Number	Evaporation Temperature (°C)	Evaporation Pressure (kPa)	Condensation Temperature (°C)	Condensation Pressure (kPa)	Pressure Ratio	Frequency (Hz)
Experiment 1	0	813.1	29	1878.0	2.31	50
Experiment 2	3	894.1	33	2081.9	2.31	50
Experiment 3	5	951.5	35	2189.8	2.31	50
Experiment 4	0	813.1	35	2189.8	2.73	50
Experiment 5	3	894.1	39	2418.4	2.73	50
Experiment 6	5	951.5	42	2601.4	2.73	50
Experiment 7	0	813.1	42	2601.4	3.20	50
Experiment 8	3	894.1	46	2861.6	3.20	50
Experiment 9	5	951.5	48	2998.9	3.20	50
Experiment 10	3	894.1	46	2861.6	3.20	40
Experiment 11	3	894.1	46	2861.6	3.20	60

In each experimental group, the opening of the electronic expansion valve is adjusted to vary the compressor's suction superheat from around 10 K to near 1 K. Subsequently, the flow state of the refrigerant within visual tube 12 at the evaporator outlet is promptly observed, and the data acquisition interface is monitored simultaneously. The presence of a mist-like flow indicates that the compressor is undergoing wet compression. The opening of the electronic expansion valve is further increased to gradually reduce the suction quality to approximately 0.88. Each experimental condition should be stabilized for 60 min with fluctuations within an acceptable range to ensure data accuracy. The data are recorded and averaged over 10 min.

2.3. Calculation Formula

The related refrigerant physical properties, such as saturated liquid enthalpy, saturated gas enthalpy, the saturation temperature of the refrigerant corresponding to the evaporator outlet pressure, and the enthalpy value before the electronic expansion valve, can be obtained through Refprop9.0. The required parameters are calculated using the above data.

Suction and discharge pressure ratio of compressor:

$$\mathrm{P}_r = P_c / P_e \tag{1}$$

The water-side cooling capacity can be expressed as:

$$Q = q_{v,w} \cdot \rho_w \cdot c_w \cdot (T_{w,i} - T_{w,o}) \tag{2}$$

In Equation (2), the flow through the evaporator water temperature change is small; so, the water density is considered to have a constant value of 1×10^3 kg·m^{-3}. The water-specific heat capacity is also considered to have a constant value of 4.2 kJ·(kg·°C)$^{-1}$.

Enthalpy of compressor suction:

$$h_{suc} = Q \cdot 1000/m + h_v \tag{3}$$

Specific entropy of compressor suction:

$$s_{suc} = f(h_{suc}, P_e) \tag{4}$$

Isentropic compression discharge enthalpy:

$$h_{dis,is} = f(s = s_{suc}, P_c) \tag{5}$$

Vapor quality of compressor suction:

$$x = (h_{suc} - h_v)/(h_{e,\,v} - h_{e,\,l}) \tag{6}$$

The suction state is superheated when the suction vapor quality x is greater than 1. The suction superheat degree is calculated as:

$$T_{\mathrm{sh}} = T_{suc} - T_e \tag{7}$$

Electrical efficiency of compressor:

$$\eta_{el} = (h_{dis,\,is} - h_{suc})/W \tag{8}$$

3. Results and Discussion

Due to the significant impact of indicator efficiency on the electrical efficiency of the compressor, the variations in operating parameters and indicator efficiency can explain the experimental phenomena and results. In reference [30], a model for the electrical efficiency of a rolling piston compressor is proposed, with the following calculation formula for the indicator efficiency:

$$\eta_i = \frac{\lambda_T \cdot \lambda_D}{1 - \frac{1.5 \cdot \Delta P_{dm} \cdot \mathrm{Pr}^{-1/k} \cdot v_{suc}}{h_{dis} - h_{suc}}} \tag{9}$$

In Equation (9), λ_T represents the temperature coefficient, λ_D represents the leakage coefficient, $\triangle P_{dm}$ represents the average pressure drop across the discharge valve, Pr represents the compression ratio of the compressor, k represents the adiabatic index of the working fluid, *such* represents the specific volume of the suction gas, and h_{dis} and h_{suc} represent the specific enthalpy of the discharge and suction gases, respectively. From Equation (9), it can be seen that the indicator efficiency is inversely proportional to the compression ratio Pr and directly proportional to the specific volume of the suction gas, v_{suc}.

It can be seen from Figure 3 that under the various experimental conditions, the compressor electrical efficiency decreases with the change in the compressor suction state (from the superheated suction to the wet compression stage). In the superheated suction section of the compressor, the electrical efficiency shows a linear downward trend, but the decrease is small. In the wet compression section, the electrical efficiency also changes linearly and decreases with the decrease in suction dryness. However, the decline is higher than that of the superheated section; that is, when the compressor is wet compressed, the compressor's electrical efficiency decreases even more. In general, the electric efficiency of the compressor decreases from superheated suction to wet compression by 5~8%. Therefore, the suction state of the compressor has a significant effect on the electrical efficiency.

When the compressor operates under the same suction state condition, a higher compression ratio results in lower electrical efficiency. On average, Experiments 1, 2, and 3 have an electrical efficiency that is 7.5% higher than Experiments 4, 5, and 6. Additionally, compared to Experiments 7, 8, and 9, the electrical efficiency is roughly 12.5% higher on average, indicating a significant effect. This is because higher compression ratios result in increased return flow and leakage, which in turn lead to higher pressure losses and more useless work. As a result, the compression ratio has a significant impact on electrical efficiency.

It appears that a higher evaporating temperature results in a smaller suction volume of the compressor, which reduces its electrical efficiency under the same compression ratio conditions. Additionally, the electrical efficiency in Experiment 7 is about 5.8% higher than in Experiment 10 under the same compressor suction conditions with a higher compression ratio. Conversely, the electrical efficiency in Experiment 1 is approximately 2.8% higher

than in Experiment 3 with a lower compression ratio. In summary, the electrical efficiency of the compressor is greatly impacted by the evaporation temperature, especially when the compressor has a higher compression ratio. Therefore, it is important to consider the influence of evaporation temperature on electrical efficiency.

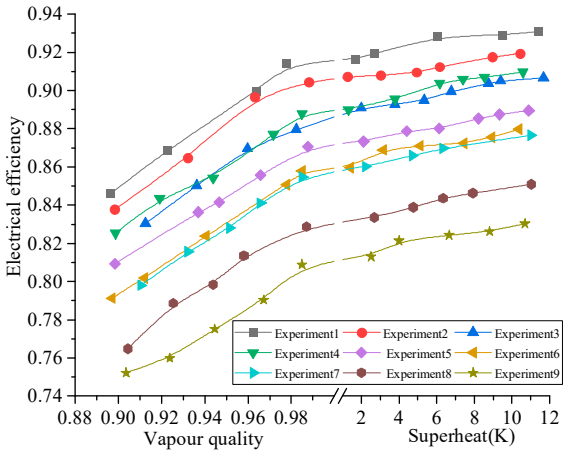


Figure 3. Variation in electrical efficiency under different working conditions at fixed frequency.

From the data presented in Figure 4, it is evident that the electrical efficiency of the compressor follows a similar trend at various frequencies. The rate of change in the superheated compressor suction and in the wet compression section remains constant. Interestingly, the data also reveal that as the compressor frequency increases, the electrical efficiency decreases for the same suction state. Experiment 10 exhibits an average compressor electrical efficiency that is 2.6% higher than Experiment 8 and 4.6% higher than Experiment 11. This could be because when the compressor runs at low frequencies, it has more time to compress the refrigerant in the chamber, resulting in a process that is closer to ideal compression. Conversely, in high-frequency operations, the refrigerant flow rate increases, leading to an increase in exhaust resistance and temperature and a deviation from ideal compression. It is worth noting that higher frequency operations also increase the heat transfer coefficient, resulting in increased heat loss and deviation from ideal compression [1]. On the other hand, running the compressor at a higher frequency allows the refrigerant to carry more lubricating oil into the suction–compression–discharge chamber, which improves the compressor's sealing performance and reduces mechanical wear. While this can affect the compressor's electrical efficiency, it has a lower impact than the pressure loss and heat loss of the exhaust valve. Therefore, the relationship between compressor frequency and electrical efficiency is complex and significant.

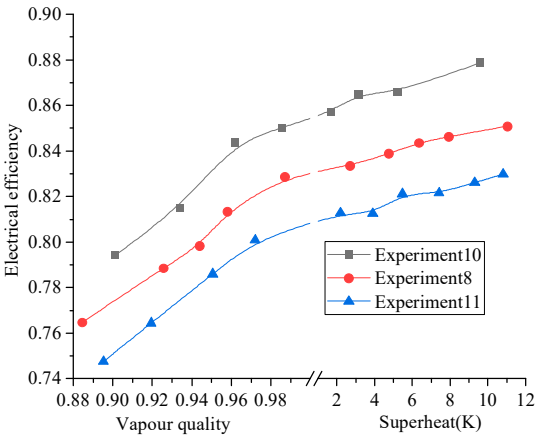


Figure 4. Variation in electrical efficiency at different frequencies under constant pressure ratio working conditions.

4. Modeling of the Electrical Efficiency for the Rolling Piston Compressor

The isentropic efficiency theoretical power and electrical power are used to evaluate the effective utilization of motor input power. This metric is influenced by several factors, including the indicated efficiency, heating efficiency, leakage efficiency, and mechanical efficiency [30].

The efficiency of the cycle is determined by comparing the input power of the actual cycle to that of the theoretical cycle. According to Equation (9), several parameters, including the temperature coefficient, leakage coefficient, compressor suction, discharge air pressure ratio, and compressor suction-specific volume c, are related to the indicated efficiency. The temperature coefficient is linked to the pressure ratio [30], while the suction-specific volume can be calculated using the evaporation temperature and the suction superheat. If there is a superheated compressor suction port, the leakage coefficient is primarily influenced by the pressure ratio. To sum up, the compressor's indicated efficiency is related to the pressure ratio, evaporation temperature, and suction superheat.

The measurement of heating efficiency is a crucial factor that indicates the amount of heat loss during the suction process. To estimate the heating efficiency, a temperature coefficient is commonly utilized. It is important to note that the temperature coefficient serves as an approximation for the heating efficiency and should be carefully considered in any heating-related analysis or evaluation. Leakage efficiency is a measure of the energy lost due to cylinder leakage, which is estimated by the leakage coefficient. This parameter is influenced by the pressure ratio in the superheated compressor suction stage. Mechanical efficiency, on the other hand, accounts for the impact of frictional power, which is primarily affected by the viscosity of the lubricant and refrigerant and is thus dependent on the mixture's temperature and concentration. In the superheated suction stage, the lubricant shows low solubility in the gaseous refrigerant, making mechanical efficiency a constant value.

Through the above analysis, it can be seen that under the same compressor frequency, when the compressor suction is superheated, the compressor electrical efficiency can be approximately equal to the function of the evaporation temperature, the suction superheat degree, and the suction and discharge air pressure ratio; that is,

$$\eta_{el} = f(T_e, T_{sh}, \mathrm{Pr}) \tag{10}$$

We can analyze the data shown in Figure 3 to show that the compressor electrical efficiency is linear with the suction superheat, i.e., when the evaporation temperature and the suction superheat are constant, Equation (10) can be simplified to Equation (11).

$$\eta_{el} = a + b \cdot T_{sh} \tag{11}$$

where a and b are constants. When the evaporation temperature and the suction superheat are not fixed, the constant b in Equation (11) is reduced to a quadratic polynomial related to the evaporation temperature and the suction superheat.

$$\begin{aligned} \eta_{el} = a_0 + \Big(a_1 + a_2 \cdot T_\mathrm{e} + a_3 \cdot \mathrm{Pr} + a_4 \cdot {T_\mathrm{e}}^2 + a_5 \cdot \mathrm{Pr}^2 \\ + a_6 \cdot T_e \cdot \mathrm{Pr}\Big) \cdot T_{sh} \end{aligned} \tag{12}$$

Equation (12) is the compressor electrical efficiency model for suction superheat at the same compressor frequency.

From Figures 3 and 4, in the wet compression section, the compressor electrical efficiency and suction dryness are in a linear relationship, and in different frequencies, they are under basically the same slope; so, the wet compression according to the compressor electrical efficiency model is:

$$\eta_{el,\,x} = \eta_{el,\,x} = 1 - a(1 - x) \tag{13}$$

According to the study in [21], a method was proposed for the construction of a performance model for variable-frequency compressors. This method involves selecting a specific frequency of the compressor as the standard frequency and standardizing both the electrical efficiency and the frequency of the compressor. The number of experiments needed is significantly reduced by implementing this model.

$$\eta_{el,\,o}/\eta_{el,\,ref} = b_0 + b_1 \cdot (N/Nref) + b_2 \cdot (N/Nref)^2 \tag{14}$$

Combining Equations (12)–(14), the rolling piston compressor electrical efficiency model can be obtained, where the standard frequency is taken as the rated frequency of 50 Hz.

The values of each fitting coefficient are obtained by fitting the data in Figures 3 and 4, as shown in Table 3.

Table 3. Fitted coefficient values.

Fitting Coefficient	Fitted Value
a_0	8.67712×10^{-1}
a_1	1.97702×10^{-3}
a_2	4.24625×10^{-4}
a_3	9.98913×10^{-3}
a_4	-4.96317×10^{-5}
a_5	-3.27234×10^{-3}
a_6	-3.89045×10^{-4}
a	7.20532×10^{-1}
b_0	1.1781
b_1	-2.2302×10^{-1}
b_2	4.4781×10^{-2}

5. Model Validation

To verify the accuracy of the rolling piston electrical efficiency model, the verification experiments under different conditions are designed. The chilled water outlet temperature, cooling water outlet temperature, and subcooling degree are set as 7 °C, 40 °C, and 5 °C, respectively. When the compressor frequency is 40 Hz, 50 Hz, and 60 Hz, the electronic expansion valve opening is adjusted to change the refrigerant from the superheated degree of 10 K to the suction dryness of about 0.88 at the compressor suction port, which means that the state of the compressor suction port is changed from the superheated state to the two-phase state.

Based on the results shown in Figure 5, it is evident that in the superheated compressor suction section during the validation conditions, the suction-to-discharge pressure ratio decreases as the suction superheat decreases. This decrease is due to the increasing of the opening of the electronic expansion valve. In contrast, the suction-to-discharge pressure ratio remains relatively stable in the compressor wet compression section. While Equation (13) assumes a constant pressure ratio for the compressor electrical efficiency model during wet compression, the data in Figure 5 validate that this assumption holds for the compressor wet compression section. Therefore, the compressor electrical efficiency model can be confidently applied under the validation conditions.

Figure 6 shows the comparison between the actual electrical efficiency and the model-calculated electrical efficiency for the compressor operating at three frequencies under the validation conditions. The results show that the maximum relative error between the calculated and the actual values of the compressor electrical efficiency model is 1.81% and that the minimum relative error is 0.035%. Therefore, the compressor electrical efficiency model is more reliable.

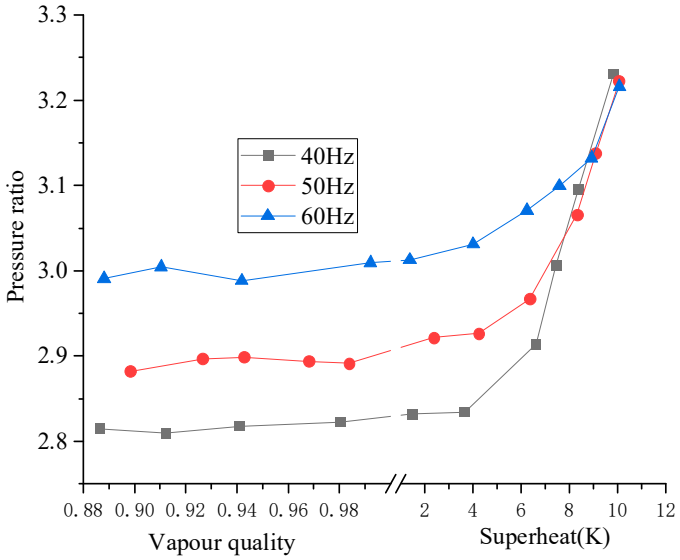


Figure 5. Verifying the change in compressor suction and discharge pressure ratio under different frequencies of working conditions.

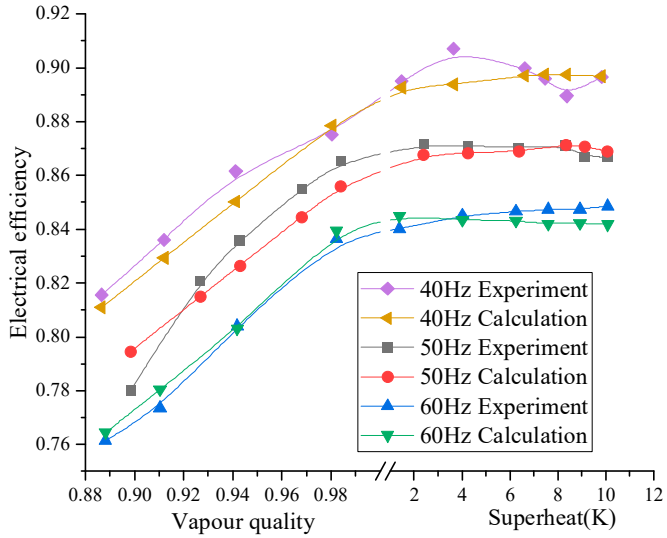


Figure 6. Experiment and calculation electrical efficiency at 40 Hz/50 Hz/60 Hz compressor frequency.

The analysis of the data shows that the maximum relative error occurs at a compressor frequency of 40 Hz and that the minimum relative error occurs at a compressor frequency of 60 Hz. This indicates that the model is more accurate at higher frequencies. During low-frequency operation, the refrigerant flow rate in the compressor cavity is relatively low, and the lubricant in the oil pool at the bottom of the compressor cannot enter the bearings effectively with the refrigerant, resulting in serious air leakage and increased wear. In summary, the rolling piston compressor electrical efficiency model is suitable for operating conditions where the compressor frequency is higher than the rated frequency and the suction dryness is greater than 0.9.

6. Conclusions

In this paper, the relationship between the compressor frequency, suction, discharge pressure ratio, superheated suction, evaporation temperature, and compressor electrical efficiency is studied through the R32 rolling piston compressor experimental setup. Meanwhile, a model of electrical efficiency for the rolling piston compressor under variable suction conditions is established. The conclusions are as follows:

(1) Under the same pressure ratio and evaporation temperature, the compressor electrical efficiency with the larger opening of the electronic expansion valve has a linear downward trend, and the slope of the suction with the liquid section is greater than that of the superheated suction section; that is, in the compressor suction with liquid the compressor electrical efficiency declines to a greater extent.

(2) Under the same pressure ratio, the larger the evaporation temperature, the smaller the electrical efficiency; under the same evaporation temperature, the larger the compressor pressure ratio, the smaller the electrical efficiency. At the same time, the higher the compressor pressure ratio, the greater the influence of evaporation temperature on the electrical efficiency of the compressor.

(3) The accuracy of the rolling piston compressor electrical efficiency model is verified through operating condition tests. The results show that the maximum relative error between the calculated value and the actual value is 1.81%, and that the minimum relative error is 0.035%. This is better than the prediction error range of ±4.95% in the compressor efficiency model proposed in reference [25], and the model established in this paper considers the influence of suction gas conditions on the compressor. Therefore, the proposed compressor electrical efficiency model is more reliable.

(4) When the compressor operates at low frequencies, the actual performance of the compressor deviates further from the calculated values of the model. Additionally, when the suction dryness is low, it can lead to the occurrence of liquid slugging in the compressor, damaging its safe operation. Therefore, the rolling piston compressor electrical efficiency model applies to operating conditions where the compressor frequency is higher than the rated frequency and the suction gas dryness is greater than 0.9.

Author Contributions: Z.C., conceptualization, methodology, software, writing—original draft; L.T., conceptualization, resources, supervision, funding acquisition, writing—review and editing; L.H., visualization, writing—review and editing; Z.Y., data curation, writing—original draft. All authors have read and agreed to the published version of the manuscript.

Funding: The support from "Shanghai Key Laboratory of Multiphase Flow and Heat Transfer in Power and Engineering" (13DZ2260900) is greatly acknowledged.

Institutional Review Board Statement: Not applicable.

Informed Consent Statement: Not applicable.

Data Availability Statement: Data is contained within the article.

Conflicts of Interest: The authors declare that they have no known competing financial interests or personal relationships that could have appeared to influence the work reported in this paper.

References

1. Fernando, M.T.-O.; Navarro-Peris, E.; Barceló-Ruescas, F.; Gonzálvez-Maciá, J. Semi-empirical model of scroll compressors and its extension to describe vapor-injection compressors. Model description and experimental validation. *Int. J. Refrig.* **2019**, *106*, 308–326.
2. Byrne, P.; Ghoubali, R.; Miriel, J. Scroll compressor modeling for heat pumps using hydrocarbons as refrigerants. *Int. J. Refrig.* **2014**, *41*, 1–13. [CrossRef]
3. Ooi, K.T.; Wong, T.N. A Computer simulation of a rotary compressor for household refrigerators. *Appl. Therm. Eng.* **1997**, *17*, 65–78. [CrossRef]
4. Prater, G., Jr. Computer Modeling and simulation of stationary-vane, rolling piston refrigeration compressors. *Cmes-Comput. Model. Eng. Sci.* **2002**, *3*, 299–312.
5. Ooi, K.T. Design optimization of a rolling piston compressor for refrigerators. *Appl. Therm. Eng.* **2005**, *25*, 813–829. [CrossRef]
6. Ooi, K.T. Assessment of a rotary compressor performance operating at transcritical carbon dioxide cycles. *Appl. Therm. Eng.* **2008**, *28*, 1160–1167. [CrossRef]
7. Ooi, K.T.; Lee, H.Q. Multi-objective design optimization of a rotary compressor for household air-conditioning. *Proc. Inst. Mech. Eng. Part E J. Process Mech. Eng.* **2008**, *222*, 241–250. [CrossRef]
8. Wu, J.; Hu, J.; Chen, A.; Mei, P.; Zhou, X.; Chen, Z. Thermal analysis for hermetic R32 rolling piston compressor. *Hsi-Chiao Tung Ta Hsueh/J. Xi'an Jiaotong Univ.* **2015**, *49*, 14–18.

9. Cai, D.; He, G.; Yokoyama, T.; Tian, Q.; Yang, X.; Pan, J. Simulation and comparison of leakage characteristics of R290 in rolling piston type rotary compressor. *Int. J. Refrig.* **2015**, *53*, 42–54. [CrossRef]
10. Farkas, B.; Szente, V.; Suda, J.M.A. Simplified modeling approach for rolling piston compressors. *Period. Poly-Tech. Mech. Eng.* **2015**, *59*, 94–101. [CrossRef]
11. Cai, D.; Qiu, C.; Pan, J.; Yang, X.; He, G.; Tetsuhide, Y.; Chen, X.; Li, H. Leakage characteristics and an updated volumetric efficiency prediction model of rolling piston type rotary compressor for small capacity air-conditioner and heat pump applications. *Appl. Therm. Eng.* **2017**, *121*, 1080–1094. [CrossRef]
12. Min, B.; Na, S.; Yang, J.; Choi, G. Geometric correlation of discharge coefficients for discharge valve system in rolling piston rotary compressor. *J. Mech. Sci. Technol.* **2018**, *32*, 3943–3954. [CrossRef]
13. Engel, R.C.; Deschamps, C.J. Comparative analysis between the performances of reciprocating and rolling piston compressors applied to a domestic heat pump water heater. *Int. J. Refrig.* **2019**, *102*, 130–141. [CrossRef]
14. Bacak, A.; Pınarbaşı, A.; Dalkılıç, A.S. A 3-D FSI simulation for the performance prediction and valve dynamic analysis of a hermetic reciprocating compressor. *Int. J. Refrig.* **2023**, *150*, 135–148. [CrossRef]
15. Roskosch, D.; Venzik, V.; Atakan, B. Thermodynamic model for reciprocating compressors with the focus on fluid dependent efficiencies. *Int. J. Refrig.* **2017**, *84*, 104–116. [CrossRef]
16. Ossorio, R.; Navarro-Peris, E. Testing of Variable-Speed Scroll Compressors and their inverters for the evaluation of compact energy consumption models. *Appl. Therm. Eng.* **2023**, *230*, 120725. [CrossRef]
17. *DIN EN 12900:2013-10*; October 2013: Kältemittel-Verdichter–Nennbedingungen, Toleranzen und Darstellung von Leistungsdaten des Herstellers. Deutsches Institut fur Normung E.V.: Berlin, Germany, 20 October.
18. AHRI Standard 540, 2015: Performance Rating Of Positive Displacement Refrigerant Compressors and Compressor Units. Available online: www.ahrinet.org (accessed on 15 March 2022).
19. Wan, H.; Cao, T.; Hwang, H.; Chang, S.-D.; Yoon, Y.-J. Machine-learning-based compressor models: A case study for variable refrigerant flow systems. *Int. J. Refrig.* **2021**, *123*, 23–33. [CrossRef]
20. Li, W. Simplified steady-state modeling for hermetic compressors with a focus on extrapolation. *Int. J. Refrig.* **2012**, *35*, 1722–1733. [CrossRef]
21. Li, W. Simplified steady-state modeling for variable speed compressor. *Appl. Therm. Eng.* **2013**, *50*, 318–326. [CrossRef]
22. Molinaroli, L.; Joppolo, C.M.; De Antonellis, S. A semi-empirical model for hermetic rolling piston compressors. *Int. J. Refrig.* **2017**, *79*, 226–237. [CrossRef]
23. Sun, H.; Hu, H.; Wu, J.; Ding, G.; Li, G.; Wu, C.; Wang, X.; Lv, Z. A theory-based explicit calculation model for variable speed scroll compressors with vapor injection. *Int. J. Refrig.* **2018**, *88*, 402–412. [CrossRef]
24. Santos, G.Z.; Ronzoni, A.F.; Hermes, C.J.L. Performance characterization of small variable-capacity reciprocating compressors using a minimal dataset. *Int. J. Refrig.* **2019**, *107*, 191–201. [CrossRef]
25. Guth, T.; Atakan, B. Semi-empirical model of a variable speed scroll compressor for R-290 with the focus on compressor efficiencies and transferability. *Int. J. Refrig.* **2023**, *146*, 483–499. [CrossRef]
26. Sun, J.; Kuruganti, T.; Munk, J.; Dong, J.; Cui, B. Low global warming potential (GWP) refrigerant supermarket refrigeration system modeling and its application. *Int. J. Refrig.* **2021**, *126*, 195–209. [CrossRef]
27. Seong, K.; Lee, D.; Lee, J. The Effects of Wet Compression by the Electronic Expansion Valve Opening on the Performance of a Heat Pump System. *Appl. Sci.* **2017**, *7*, 248. [CrossRef]
28. Itard, L.C.M. Wet compression versus dry compression in heat pumps working with pure refrigerants or non-azeotropic mixtures. *Int. J. Refrig.* **1995**, *18*, 495–504. [CrossRef]
29. Vorster, P.P.J.; Meyer, J.P. Wet compression versus dry compression in heat pumps working with pure refrigerant or non-azeotropic binary mixtures for different heating application. *Int. J. Refrig.* **2000**, *23*, 292–311. [CrossRef]
30. Ding, G.; Zhang, C. *Simulation and Optimization of Refrigeration and Air Conditioning Units*, 1st ed.; Science Press: Beijing, China, 2001. (In Chinese)

Disclaimer/Publisher's Note: The statements, opinions and data contained in all publications are solely those of the individual author(s) and contributor(s) and not of MDPI and/or the editor(s). MDPI and/or the editor(s) disclaim responsibility for any injury to people or property resulting from any ideas, methods, instructions or products referred to in the content.